

Article

The Pelagic Habitat of Swordfish (*Xiphias gladius*) in the Changing Environment of the North Indian Ocean

Thushani Suleka Madhubhashini Elepathage ^{1,2,3,4} , Danling Tang ^{1,2,4,*} and Leo Oey ⁵

¹ LTO, Guangdong Key Laboratory of Ocean Remote Sensing, South China Sea Institute of Oceanology, Chinese Academy of Sciences, Guangzhou 510301, China; thushanis@pdn.ac.lk

² University of Chinese Academy of Sciences, Beijing 100049, China

³ Department of Animal science, Faculty of Agriculture, University of Peradeniya, Peradeniya 20400, Sri Lanka

⁴ Southern Marine Science and Engineering Guangdong Laboratory, Guangzhou 510301, China

⁵ Sayre Hall, 300 Forrestal Road, Princeton University, Princeton, NJ 08544, USA; lyo@princeton.edu

* Correspondence: lingzistdl@126.com

Received: 17 October 2019; Accepted: 6 December 2019; Published: 10 December 2019



Abstract: Swordfish (*Xiphias gladius*) are a highly migratory keystone species, found in tropical and temperate seas that are influenced by environmental parameters. In the Bay of Bengal, the Arabian Sea, and the ocean region around Sri Lanka, the environment is gradually changing as a result of climate change. In this study, we identified the preferable environmental conditions for swordfish using satellite-derived environmental data and in-situ fish catch data. We modeled the relationships between fish distribution and the environment changes using Boosted Regression Trees (BRT) and Generalized Additive Model (GAM) methods. The monthly mean fishing effort is comparatively high from October to March and the fish catch rates are high from September to November. Chlorophyll-a concentration has a positive relationship with catch rates while sea surface temperature (SST), sea salt surface mass concentration (SSS), and effort show negative relationships. Approximately 0.3–0.4 mgm⁻³ of chlorophyll-a, 28–28.5 °C SST, and (3–5)10⁻⁸ kgm⁻³ of SSS were significantly correlated with high swordfish catch rates. According to the optimum environmental conditions identified using the above models, the suitable environmental spatial and temporal distribution was mapped. The results show that the optimum conditions for swordfish are in the eastern region of Sri Lanka, around Thailand and Myanmar, from June to August, and around Bangladesh, Myanmar, Pakistan, the west coast of Sri Lanka, and the east coast of India during September to November.

Keywords: Bay of Bengal; Arabian Sea; Sri Lanka; generalized additive model; boosted regression trees

1. Introduction

Swordfish (*Xiphias gladius*) (Figure A1 of Appendix A) is a kind of billfish that belongs to the family Xiphiidae found in tropical and temperate oceans. They are highly migratory and can grow to over 540 kg in weight and 445 cm in length [1]. Swordfish are carnivorous and adult fish feed on many types of prey such as anchovies, squid, hake, jack mackerel, rockfish, barracudas, black smelt, ribbonfish, sea birds, small sea mammals, and shrimp; while at the larval stage, they depend on zooplankton [2]. In the Indian Ocean, swordfish spawn in the coastal waters southwest of the Reunion Island (21° S, 55.5° E, east of Madagascar) during the austral spring and summer (October to April) [3], off the northwestern coast of Somalia, and in the Bay of Bengal (BoB) [4]. The main type of swordfishing gear used in the Indian Ocean is the longline [5]. High catches of swordfish have been reported during the spawning period [3].

Swordfish fishery is an important activity for the North Indian Ocean fishing industry [6]. With global warming and climate change, physical environmental parameters such as temperature [7], wind

and waves [8], and cyclone frequency [9,10] are changing significantly in the North Indian Ocean, and many fish species have been affected by these changes [11–13]. Swordfish are highly migratory and may change their habitat ranges in response to changes in the environment. The swordfish is a keystone species in the Indian Ocean [14]. The distribution change of the keystone species can significantly affect sustainable fishery management as well as the balance of the ecosystem. Some previous studies have identified the environmental variables that affect swordfish in the Atlantic Ocean [15] and the Indian Ocean [16]. Some studies identified their feeding habits and habitats [2]. However since these changes depend on the particular regions being studied [17], detailed regional studies are useful.

The present study focuses on the BoB, the ocean area around Sri Lanka and the southeastern Arabian Sea (AS). Net evaporation in the western part of the North Indian Ocean and net precipitation in the eastern part result in a salinity difference between the AS and the BoB [18]. The ecosystems of the BoB play a significant role in providing a livelihood and diet to the coastal human population of the nearby countries [19]. These ecosystems are highly productive, due to the nutrient input from rivers and from vertical mixing driven by wind, waves, and currents. In this study, we test the hypothesis that physical environmental variables influence swordfish pelagic habitats and distribution in the North Indian Ocean. The goal is to identify the quantitative ranges of the environmental variables that are correlated with swordfish distribution patterns in the BoB, the seas around Sri Lanka, and the southeastern AS.

2. Materials and Methods

2.1. Environmental Variables

The study area (Figure 1) is located between 70° E and 98.5° E longitudinally, and 0° N to 22° N latitudinally, including the BoB, the AS and the Sri Lankan Exclusive Economic Zone (EEZ). The remote sensing data of Chlorophyll-a concentration (Chl-a) and sea surface temperature (SST) at 4 km resolution were obtained from the Moderate-resolution Imaging Spectroradiometer (MODIS)-Aqua L3m. Surface wind at 0.5° × 0.667° resolution and sea salt surface (SSS) mass concentration at 0.5° × 0.625° resolution were obtained from the Modern-Era Retrospective analysis for Research and Applications, Version 2 (MERRA-2) Model. The sea surface height (SSH) and sea surface height anomaly (SSHA) were obtained from Environmental Research Division's Data Access Program (ERDDAP). Wind speed data at a 1° resolution were from the Aquarius Combined Active Passive (CAP) Level 3 products, and mixed layer depth (MLD) at 0.67° × 1.25° resolution from the NASA Ocean Biogeochemical Model (NOBM). These environmental data were monthly averaged and, together with the monthly swordfish catch per unit effort (CPUE) distribution, were used to study their seasonal co-variability.

2.2. Swordfish Fish Catch Data

We used the Indian Ocean Tuna Commission (IOTC) and the National Aquatic Resources Research and Development Agency (Sri Lanka) fisheries data from 2002 to 2015. For the detailed analysis the long line fisheries data from 2002 to 2015 were obtained from the fisheries harbors with fishing effort (number of hooks), fishing date, vessel capacity, location, and catch amount (in number of swordfish). Both daily catch data and the monthly means were used in our analysis. CPUE was calculated as a number of fish captured per 5000 hooks.

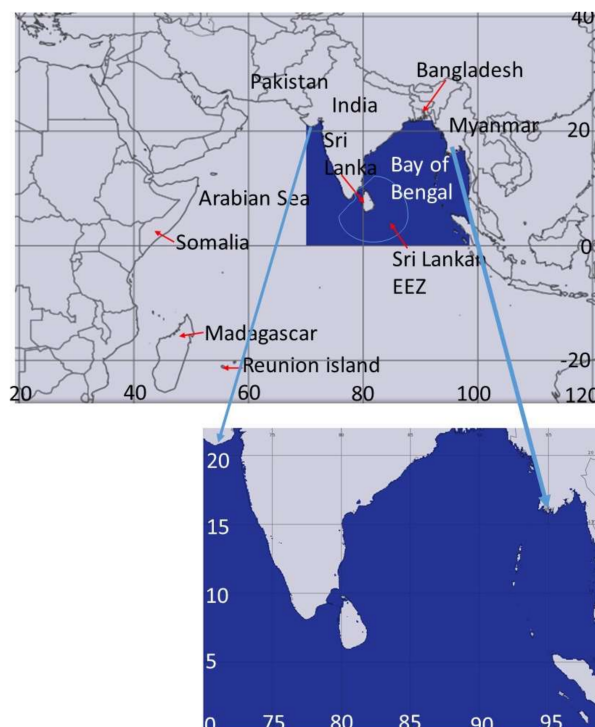


Figure 1. Study area (70° E to 98.5° E, and 0° N to 22° N) indicated in blue.

2.3. Statistical Models for Spatial Predictions of Catch Rate

Initially, Boosted Regression Trees (BRT) were used to identify the influencing parameters on swordfish catch distribution using the 'gbm' function in the 'gbm' package [20]. Boosted regression trees perform well in predictive and descriptive studies [20] and their predictive performance surpasses most traditional modelling methods [21]. The authors in reference [22] have identified that BRT performs better than the generalized linear model in climate-related studies. BRTs are really advantageous in tree-based methods, studying various types of predictor variables, and in identifying missing data [21]. In BRT, prior data transformation or elimination of outliers is not necessary [21]. The complex nonlinear relationships, and interaction effects between predictors are automatically handled by the BRT model [23]. The poor predictive performance of single tree models can be ameliorated by fitting multiple trees in BRT. The BRT can be summarized in ways that provide influential ecological insights [21].

Then the generalized additive models (GAMs) were used to predict potential swordfish pelagic spatial habitats according to the relationships between environmental variables identified with BRT and swordfish CPUEs using the 'gam' function of the mgcv package [24]. Several base models were prepared and the final model was selected according to the highest R-squared value, the least Akaike information criterion (AIC) value, generalized cross-validation (GCV) value, and the diagnostic plots (residuals distribution plot, quantile-quantile plot, and response vs. fitted values plot). GAMs deal with non-linear relationships of ecological variables well and describe the variance of a response variable effectively [25]. Both BRTs and GAMs were constructed in R (Version i386 3.4.2). The GAM formula structure is

$$\log(\text{CPUE} + c) = a_0 + s(x_1) + s(x_2) + s(x_3) + \dots s(x_n) \quad (1)$$

Here, $s(x_n)$ is the smoothing function of covariates (x_n) and a_0 is the model constant. All covariates were treated as continuous, and the effective degrees of freedom were assessed for each main factor [26]. We added 0.1(c) to all catch rates, as the log-link function is incapable of handling zeroes [27]. A constant

value of 0.1(c) can be used to standardize the catch rate of swordfish [27]. The fish CPUE and the distribution of the environmental variables were mapped using the ArcGIS 10.5 software.

3. Results

3.1. The Swordfish Catch Distribution in North Indian Ocean

The spatial and temporal distribution of the swordfish nominal CPUE (Figure 2) shows that the catch distribution is low from April to June and high from September to November. Throughout the year, high catches can be observed from 0° N to 5° N latitudes. The monthly mean variation of the effort and the catch rate of the swordfish (Figure 2) indicate comparatively high fishing effort from October to March. The fish catch rates do not show a considerable variation with the fishing effort. According to the data, longline fisheries have been operating continuously throughout the year, although there are seasonal variations.

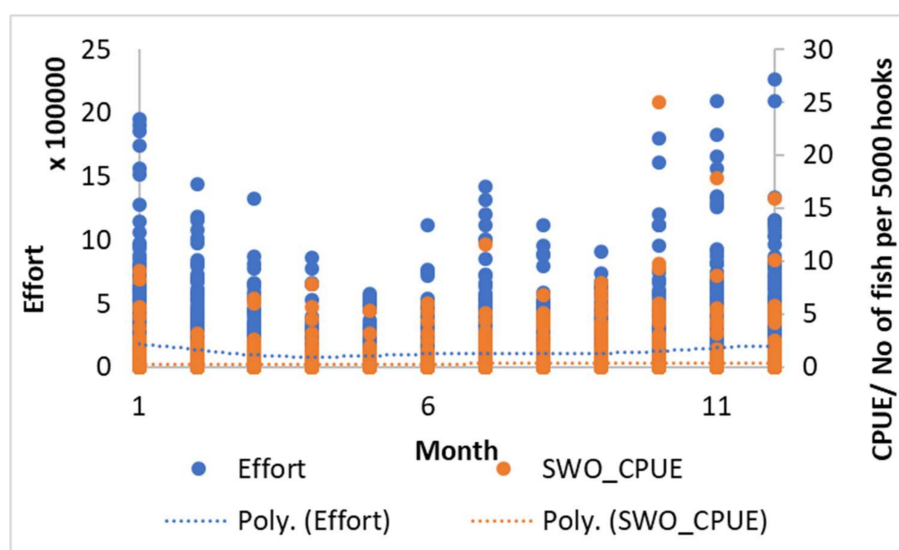


Figure 2. Monthly variations of the Swordfish (SWO) catch per unit effort (CPUE) and effort (number of hooks).

3.2. Identification of Influencing Variables for Swordfish Catches Distribution with BRT Model

Table 1 shows the selected variables and their influencing rates on the swordfish catch distribution. Variable selection in BRT is attained according to the relative influence. The model basically ignores non-informative predictors while fitting trees. Hence, the results are fairly reasonable as the measures of relative influence compute the importance of predictors, and irrelevant ones have a minimal effect on prediction [21]. The relative influence of predictor variables is estimated by the formulae developed by reference [28] and implemented in the gbm library. The measures are grounded on the number of times a variable is selected for splitting, weighted by the squared improvement to the model as a result of each split, and averaged over all trees [29].

The total number of observations used in the BRTs and GAMs was 3887. Out of them, 3685 data were less than or equal to 1 swordfish catch per 5000 hooks. According to the relative influence calculated in BRT, the three main influencing variables for the swordfish catch rate are time (year) (38.16%), SST (10.89%) and chl-a concentration (10.28%). Longitude (2%) and latitude (0.41%) have the least relative influence. Thus, inter-annual variations have a dominant influence on CPUE, as shown in Figure 3, which plots the nonlinear changes of the identified parameters with the CPUEs. Fitted functions for main effects of the swordfish CPUE, by influencing variables in the BRT model, are indicated as a plot in Figure 3.

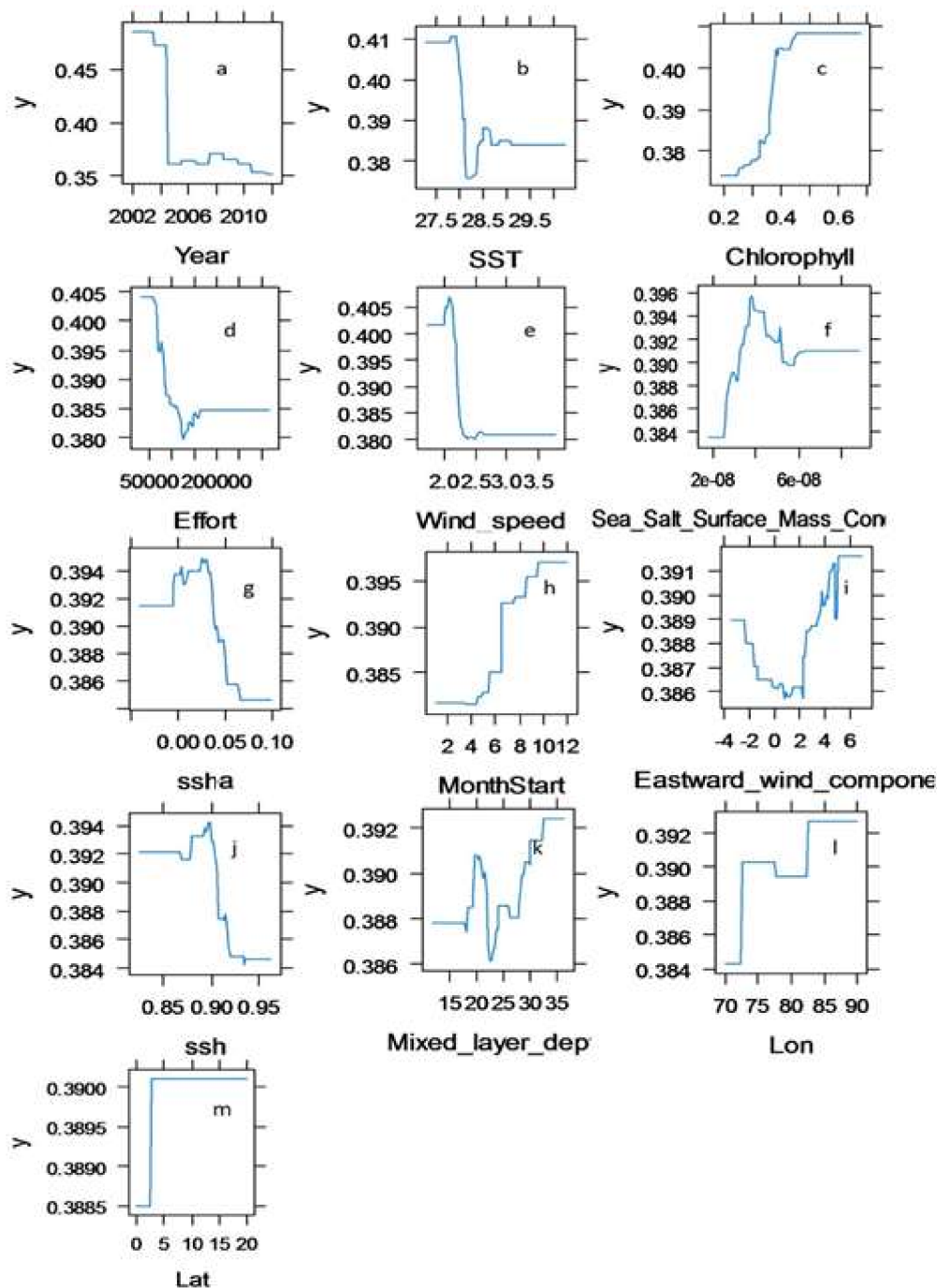


Figure 3. Fitted functions for main effects of the swordfish CPUE (y) in the BRT model. (a) Year. (b) Chlorophyll-a. (c) SST. (d) Effort. (e) Wind speed. (f) Mixed layer depth. (g) SSHA. (h) SSS mass concentration. (i) Month. (j) SSH. (k) Eastward wind component. (l) Longitude (Lon). (m) Latitude (Lat).

According to the results of the BRT model (Figure 3) 28–28.5 °C SST, 0.3–0.4 mg m⁻³ Chl-a, 2–2.5 m s⁻¹ wind speed, (3–5)10⁻⁸ kg m⁻³ SSS mass concentration, 0.03–0.05 m SSHA, 2–5 m s⁻¹ eastward wind component, 0.9–0.92 m SSH, and 27–32 m MLD were significantly related environmental conditions with swordfish CPUE distribution. Other than the environmental variables, the factors such as the years from 2004 to 2005, 50,000–200,000 measures of effort, the June to October months, 73° E and 83° E longitudes, and 2° N latitude also show significantly strong relationships with swordfish

catch rates. In the BRT model, the location (latitude and longitude), SSH, and SSHA were significant parameters; however, in the GAM they did not show a significant contribution to the model.

Table 1. The influencing rate of the boosted regression trees (BRT) simplified model variables.

Variable	Relative Influence (%)
Year	38.16
Sea surface temperature (SST)	10.89
Chlorophyll-a	10.28
Effort	9.02
Wind speed	7.47
Sea Salt Surface Mass Concentration	4.99
Sea surface height anomaly (SSHA)	3.81
Month	3.43
Eastward wind component	3.28
Sea surface height (SSH)	3.18
Mixed layer depth	3.08
Longitude	2.00
Latitude	0.41

3.3. GAM Selection and the Influencing Variables on Swordfish Distribution

The identified variables with BRT were tested in GAMs. The details of the selected model are indicated in Table 2.

Table 2. Expected Default Frequency (Edf), reference degree of freedom (ref.df), F and *p*-values of the influencing variables in the generalized additive model (GAM) and the adjusted R-squared, deviance explained and generalized cross-validation (GCV) of the selected GAM models. Akaike information criterion (AIC).

	edf	Ref.df	F	<i>p</i> -Value		R-sq. Adjusted	Deviance Explained	GCV	AIC	
s(Year)	8.18	8.82	6.369	3.45×10^{-7}	***					
s(Month)	1	1	0.075	0.7847						
s(Effort)	1	1	4.773	0.031	*	0.33	40..30%	0.31996	214.26	Model 1
s(Chl-a)	1	1	5.992	0.0159	*					
s(SST)	1	1	5.897	0.0167	*					
s(Sea Salt)	1	1	1.733	0.1907						

Significance codes: 0 *** 0.001 ** 0.01 *.

Out of many models prepared with GAM, model 1 was selected as the best model as it had a comparatively high deviance explained (40.3%) and R^2 value (0.33), and the lowest Akaike information criteria (AIC) (214.26) and generalized cross-validation (GCV) value (0.31996). R^2 is the percentage of the total variation of the dependent variable accounted by the independent variables. An R^2 value close to 1 indicates that the data perfectly fit the model [30]. GCV is an estimate of the parameters in the context of inverse problems and regularization techniques. It determines the smoothness parameter in splines [31,32]. AIC is an estimator of the relative quality of statistical models. The model with the lowest AIC can be considered as the best model [33,34]. Log (CPUE) were used in both models because the log transformation made the data normalized. Quintile–quintile plots of both models indicated that the distributions of residuals confirm the assumption of a Gaussian distribution. The year and month were contributed to the model as a spline parameter. The year was a major contributor in the model (*p*-values 3.45×10^{-7}). Effort (0.031), SST (0.0167), and Chl-a (0.0159) were also significant variables. The location (longitude and latitude) did not contribute in the model to increase the deviance explained or the adjusted R-squared values. The modeled effect of environmental variables on catch rates according to model 1 is shown in Figure 4.

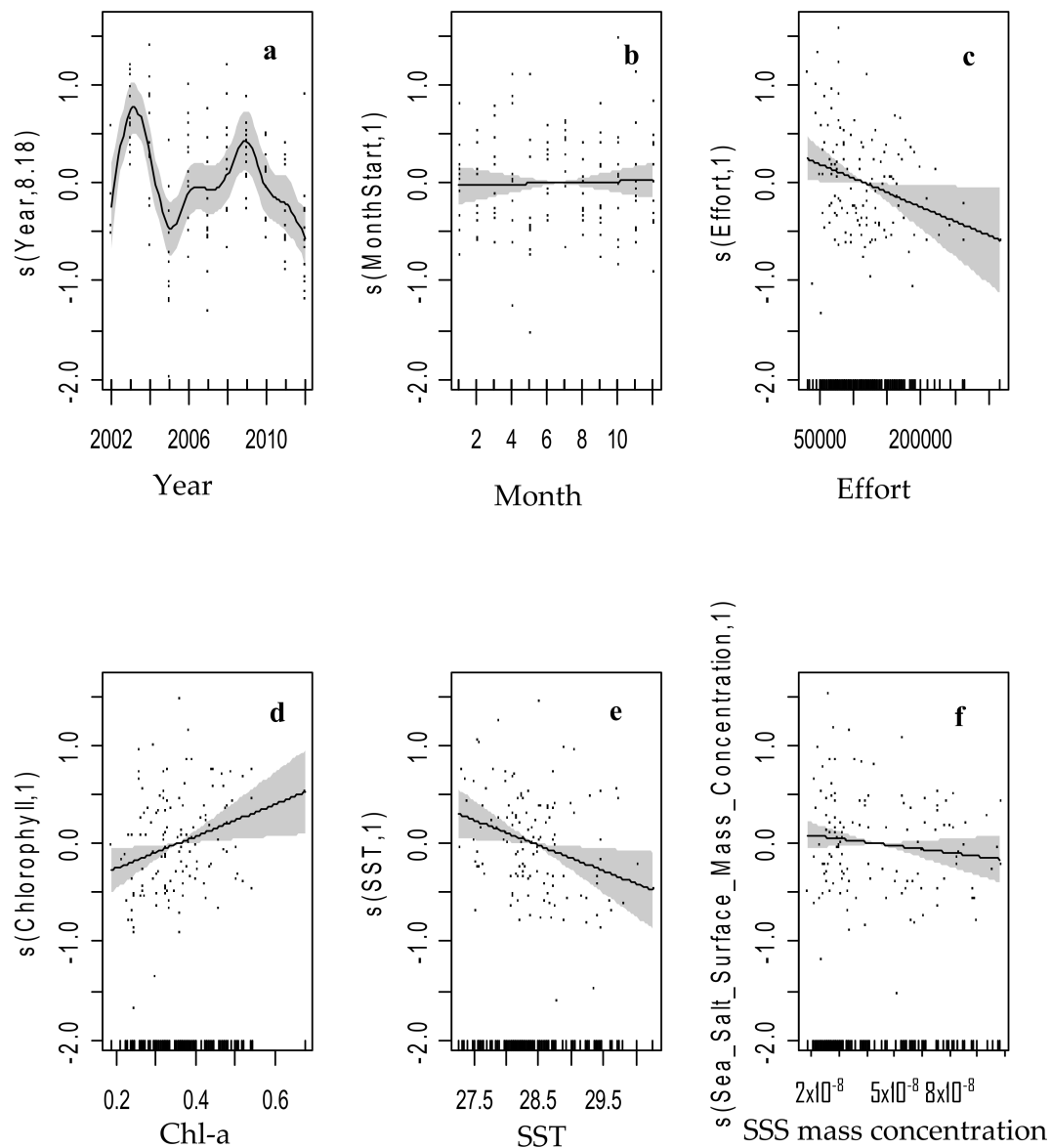


Figure 4. Modeled effect of (a) year, (b) month, (c) effort, (d) Chlorophyll-a, (e) SST, and (f) sea surface salt (SSS) mass concentration on swordfish catch rates in the study region. The black solid line indicates the fitted GAM function and the ash color area indicates 95% confidence intervals. The relative density of data points is shown by the rug plot on the x-axis and the data are indicated by black dots.

After considering the significance of AIC, GCV, and R-square values, model 1 was selected for further examination. According to model 1, Chl-a and the month show positive relationships with catch rates while SST, SSS mass concentration, and effort show negative relationships with CPUE. Approximately $0.3\text{--}0.4\text{ mg m}^{-3}$ of Chl-a (Figure 4d), $28\text{--}28.5\text{ }^{\circ}\text{C}$ SST (Figure 4e) and $(3\text{--}5)10^{-8}\text{ kg m}^{-3}$ of SSS mass concentration (Figure 4f) were significantly correlated with the swordfish catch rates. Other than these environmental variables, 75,000–150,000 hooks, the June–November months, and the years 2003–2005 are significant in the GAM model.

3.4. Inter-Annual and Seasonal Variability of the Environmental Variables

According to the inter-annual variability plots and the maps (Figure 5), Chl-a (a) and Sea salt (c) have decreasing trends and SST (b) has an increasing trend during 2002–2015. The minimum CPUE during 2002–2015 was reported in 2005 (0.21) and maximum was reported in 2014 (1.01). The Chl-a has

well bloomed in 2002 (0.41 mg m^{-3}) and declined up by to 0.29 mg m^{-3} by 2015. Proving the negative relationship between Chl-a and SST the minimum SST within this period can be seen in 2002 ($28.25 \text{ }^\circ\text{C}$), and maximum, in 2015 ($28.8 \text{ }^\circ\text{C}$). The swordfish annual mean CPUE in 2002 is 0.3 and in 2015, 0.95. The minimum SSS mass concentration is shown in 2008 (4×10^{-8}) and the maximum in 2005 (4.73×10^{-8}).

According to the monthly plots (Figure 6), the peak season for swordfish catch is from September to December. This is preceded by Chl-a, which starts to increase from June and reaches a peak level in September (0.46 mg m^{-3}). The least Chl-a is in April (0.24 mg m^{-3}), when the study area experiences the highest SST ($29.47 \text{ }^\circ\text{C}$). The least SST is observed in July ($28.18 \text{ }^\circ\text{C}$). SST and SSS concentration show an inverse relationship. SSS mass concentration reaches its peak in July ($7.37 \times 10^{-8} \text{ kg m}^{-3}$) after a gradual increase starting from April, after passing its lowest level in March ($2.45 \times 10^{-8} \text{ kg m}^{-3}$).

The seasonal maps of the above variables (Figure 7) indicate comparatively high Chl-a distribution from December to May around the Pakistan, Bangladesh, and Myanmar coastal regions. The Chl-a concentration seems to be higher during December to February than from March to May. During June to August, plankton blooming is seen around the South Indian and Sri Lankan coastal regions, Thailand, and Myanmar. Chl-a shows a high density in Pakistan, Indian, and Bangladeshi coastal areas from September to November. However, during those months, the West Indian coastal region has a higher amount of Chl-a than the East Indian coast.

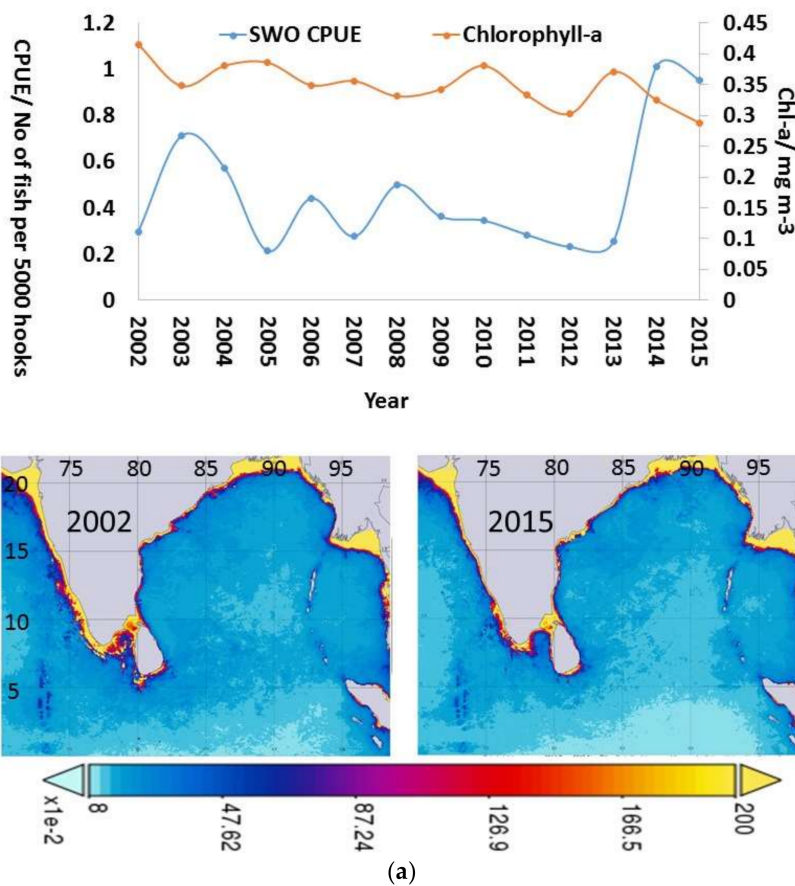


Figure 5. Cont.

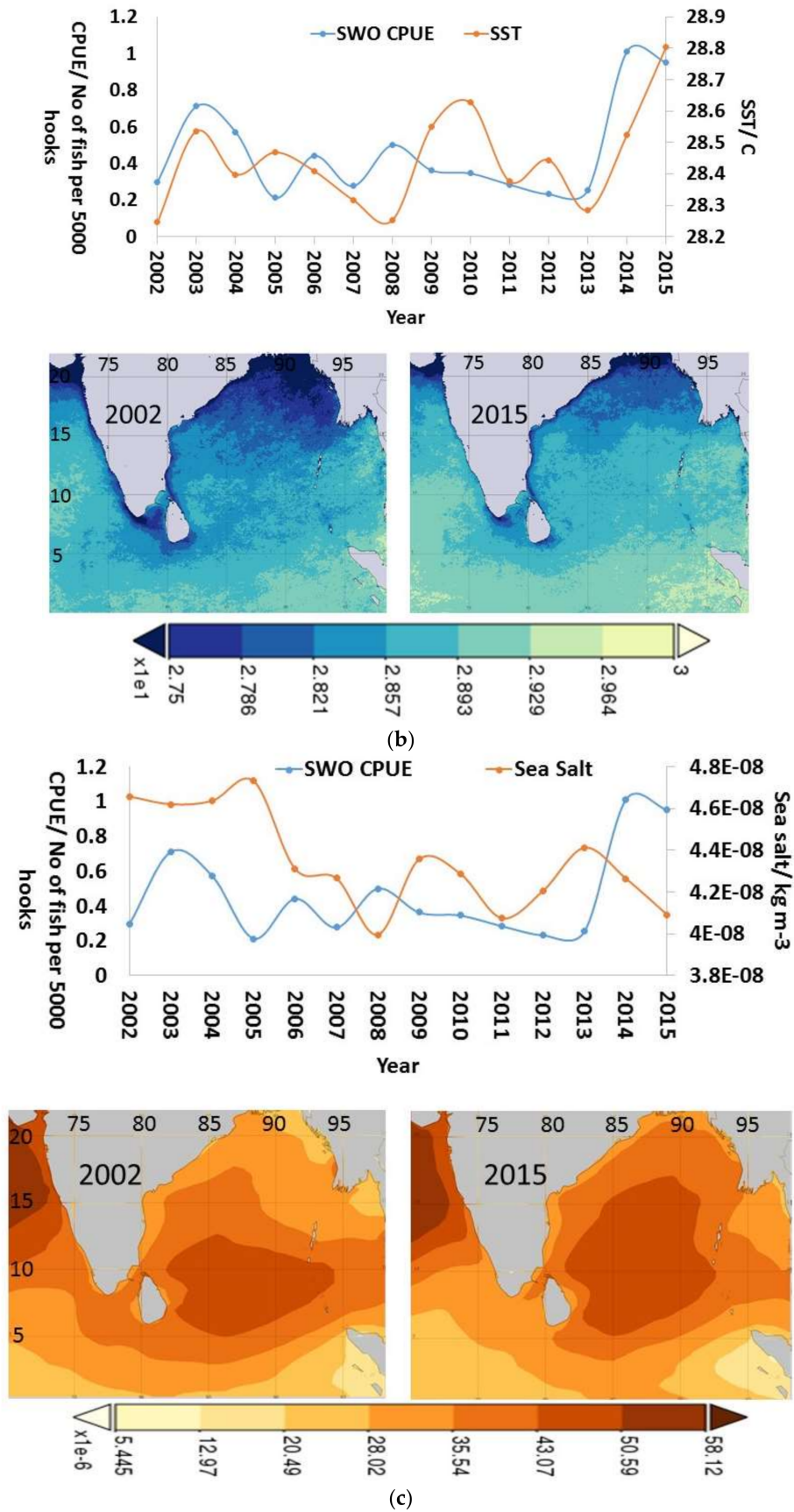


Figure 5. Inter-annual variability of the variables (a) Chl-a, (b) SST, and (c) SSS mass concentration.

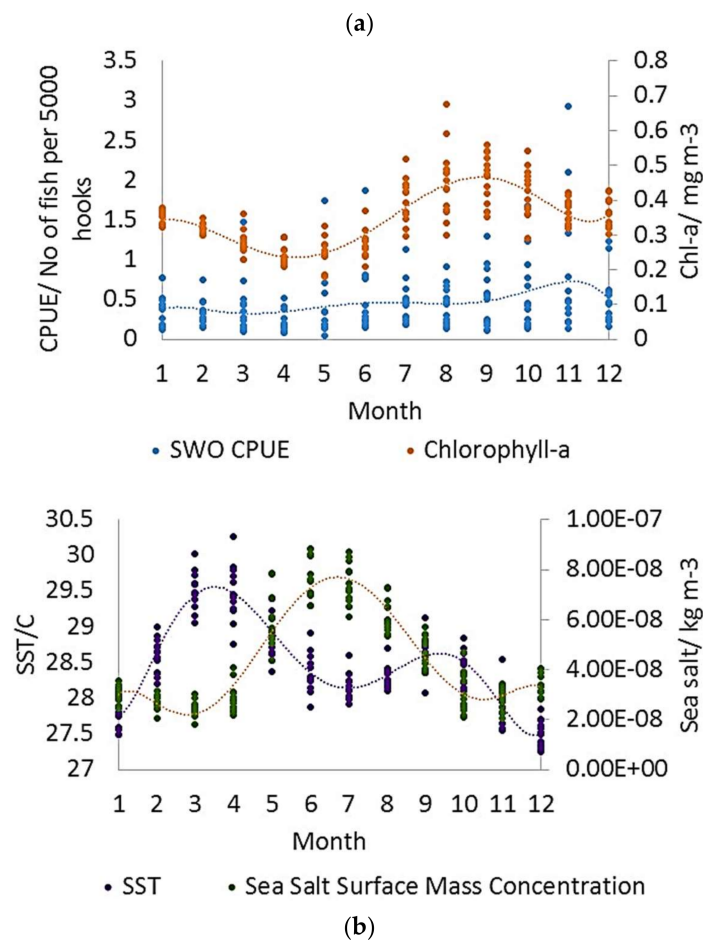


Figure 6. Monthly variations of swordfish (a) CPUE, Chl-a, and (b) SST and SSS mass concentration.

In the seasonal maps (Figure 7), the spatial and temporal distribution of high Chl-a concentrations is observed when the SST is comparatively low. Low Chl-a is seen when the SST is high. During December to February, low SST is seen in Pakistan, Bangladesh, and Myanmar coastal regions, and from March to May, the SST is high in all areas. From June to August there is a low SST distribution around the South Indian coast and Sri Lanka. From September to November low SST can be seen in Pakistan, West Indian, and Bangladesh coastal areas.

From September to February, SSS mass concentration is very high around India, and the eastern region of Sri Lankan waters shows much higher SSS than the western region. From March to May, the northeast coast of India and the coastal region of Bangladesh show high SSS mass concentration. From June to August, the Pakistan and West Indian coast show high SSS. Moreover, from June to November, there is a high SSS dome in the middle of the BoB. The SSS mass concentration increases further and reaches a maximum in September–November. During the same months, a higher SST can be observed at the edge of the high SSS dome and a lower SST is seen in the middle.

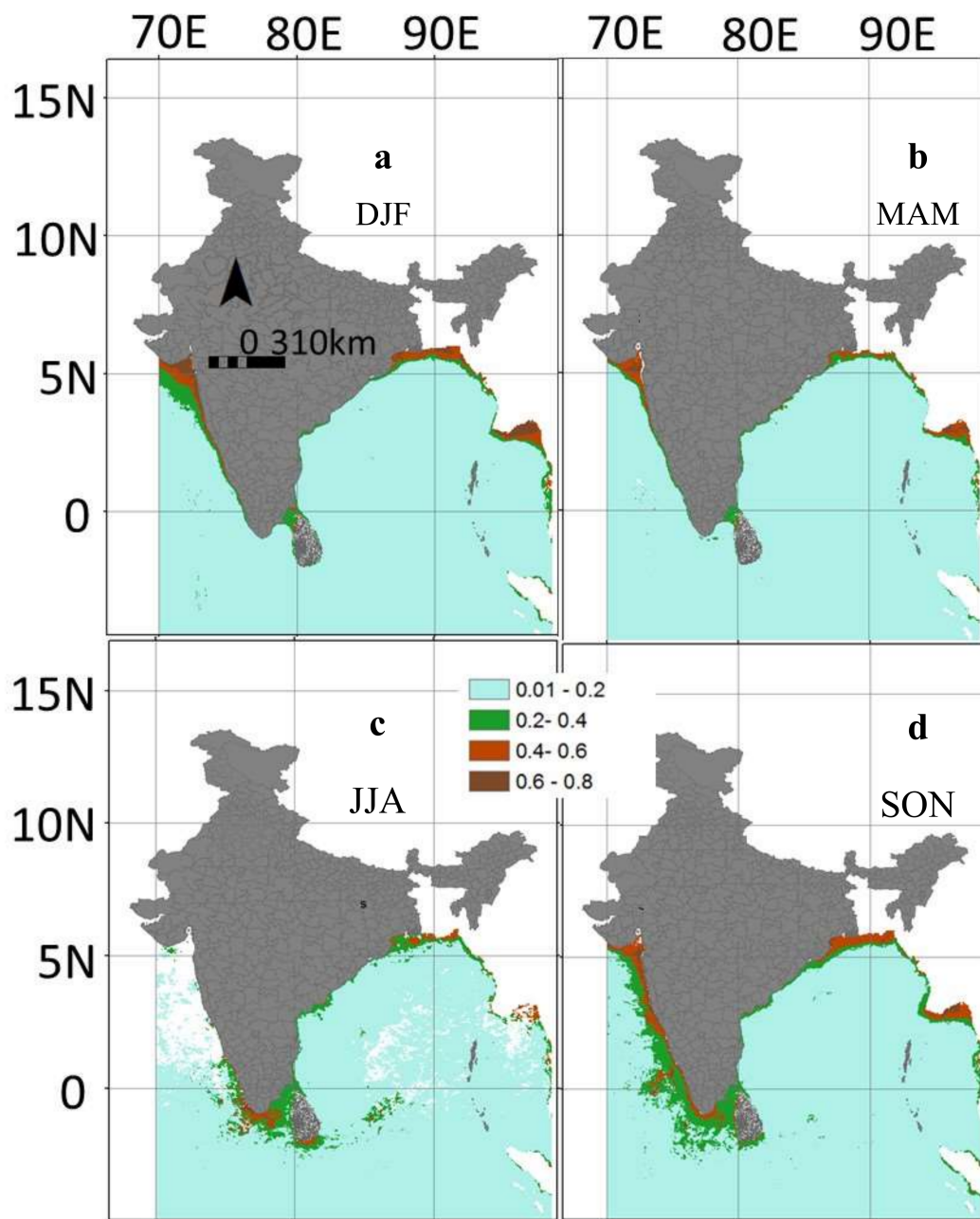


Figure 7. Cont.

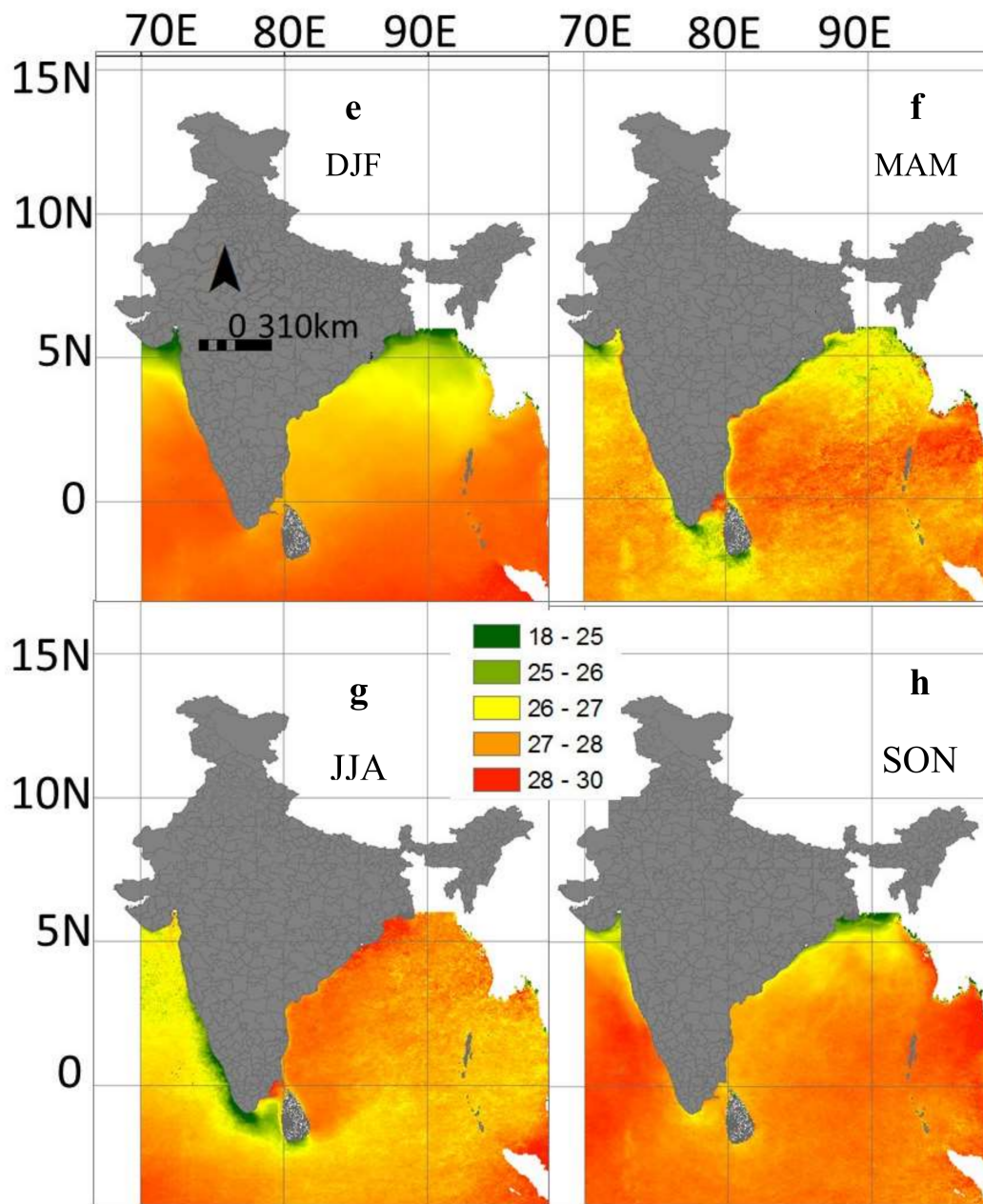


Figure 7. Cont.

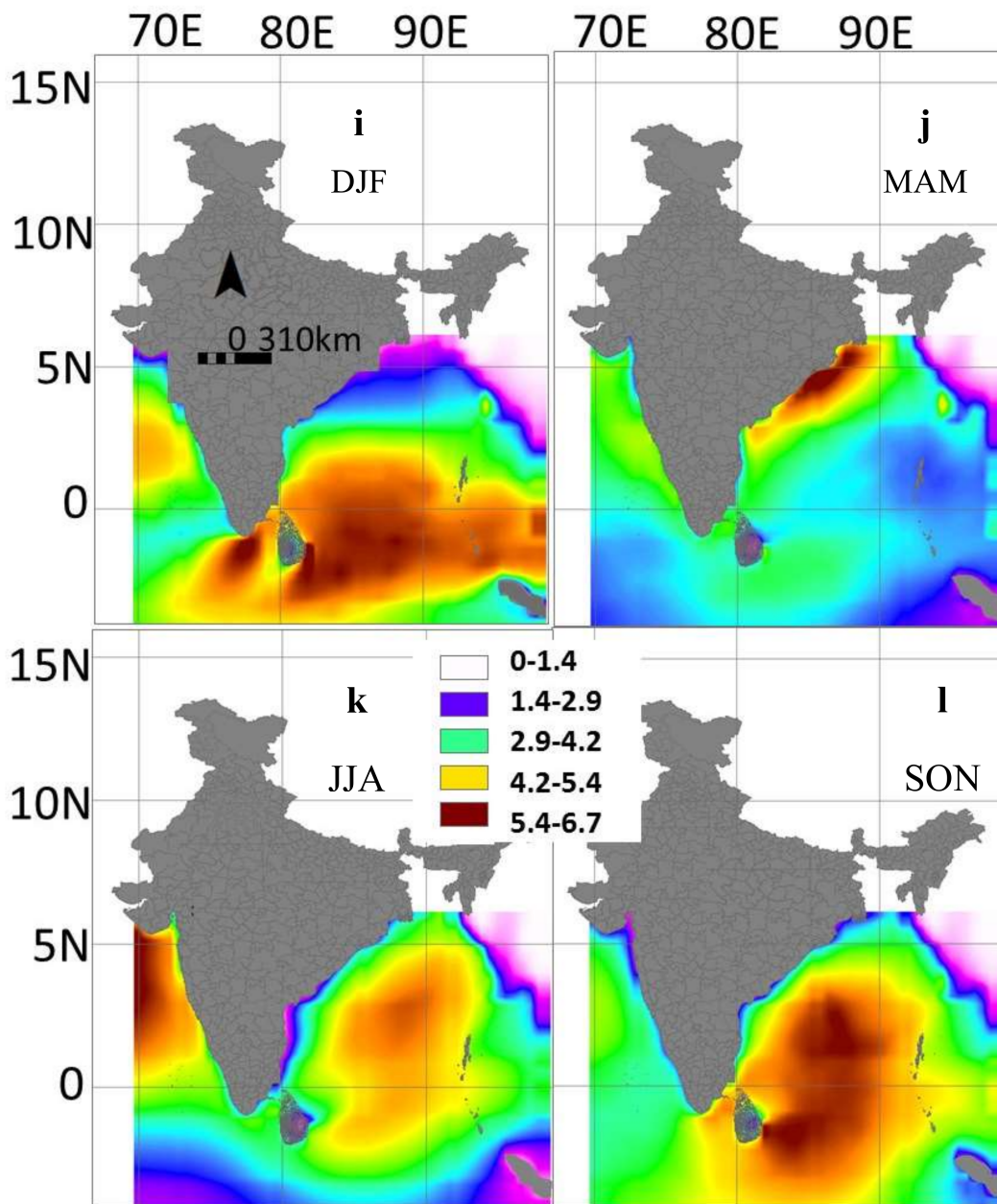


Figure 7. The seasonal change of (a–d) Chl-a (mgm^{-3}), (e–h) SST ($^{\circ}\text{C}$), and (i–l) SSS (10^{-8} kgm^{-3}). (Land masks in ash color. DJF = December–February; MAM = March–May; JJA = June–August; SON = September–November).

3.5. Predicted Spatial Distribution of Swordfish in the Indian Ocean

The optimum SST, Chl-a, and SSS mass concentration values identified with the GAM were intersected and the pelagic habitats of swordfish were mapped according to the seasonal variations of the environment (Figure 8).

According to the maps, the highest distribution of habitats can be observed from June to November. From June to August the habitats are abundant in the eastern region of Sri Lanka, India, and near the Myanmar and Thailand coasts. During September to November, the habitats are densely distributed near Pakistan, the west coast of Sri Lanka, the east coast of India, and around Bangladesh and Myanmar. The distribution of habitats is very low from March to May.

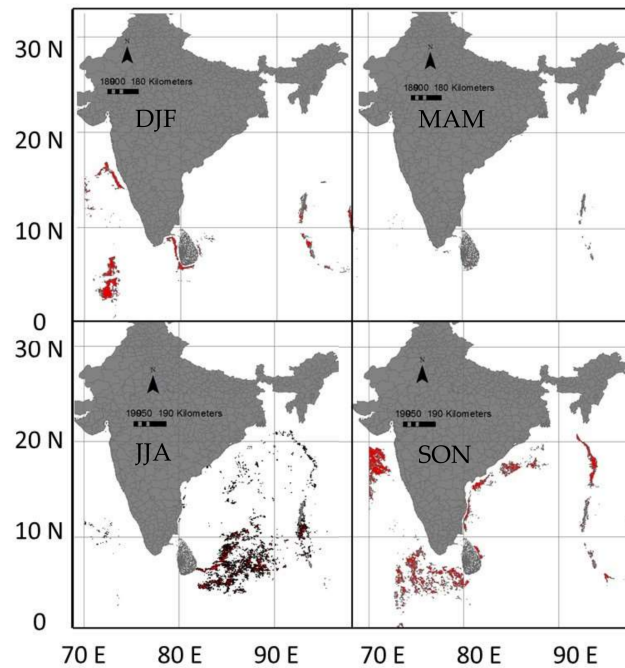


Figure 8. The pelagic habitat of swordfish according to the distribution of optimum environmental conditions. (Habitats are demarcated in red; land masks are indicated with an ash color.).

4. Discussion

4.1. Overview

In many genetic studies and stock assessment studies, physical oceanographic parameters that affect species distribution are not considered. Moreover, when the studies are conducted in small areas using only in-situ data, the correlation between the environment variables and fish distribution is unclear. The relationship between the biological components and the environment variables is expected to be non-linear. The present study was carried out using the satellite-derived environment data, in-situ fish catch data, and non-linear BRT and GAM models to identify the influencing parameters that can affect swordfish habitats.

4.2. Inter-Annual and Seasonal Changes in Environmental Variables and CPUE

The inter-annual changes (Figure 5), monthly changes (Figure 6), and seasonal changes (Figure 7) clearly indicated the negative relationship between SST and Chl-a. Moreover, there is a considerable effect from monsoons and the Indian Ocean Dipole (IOD) [16] on the seasonal and annual variations of the studied variables. From March to May, the tropical ocean waters are warm due to high solar insolation [35]. Since Chl-a and SST are inversely related [36,37], the low Chl-a spatial and temporal distributions can be observed when SST is high. According to the fisheries statistics of India, Myanmar, and Bangladesh, the peak seasons of swordfish fisheries are available in the seasons when comparatively high Chl-a is observed in those regions (Figure 8) [38,39].

The high salinity dome is visible in the middle of the BoB in the June, July, and August months due to the Sri Lankan dome created with the westerly winds [40]. The high-density saline water, high-speed wind, and low SST in this area induce well-developed upward doming isotherms, and open-ocean Ekman pumping [41]. The nutrient circulation with Ekman pumping in this area promotes phytoplankton growth (Figure 7). The phytoplankton, which contains the Chl-a pigment, influences the swordfish distribution.

According to the inter-annual changes (Figure 5), there is a considerable decrease of SST in the BoB area with the consecutive IOD events that occurred from 2006 to 2008 [42]. Within that period,

the swordfish CPUE also shows a visible fluctuation. Moreover, there is a significantly positive SST anomaly visible in 2015 due to the El Niño–Southern Oscillation (ENSO), which occurred from 2014 to 2016 [10]. With the increase of SST, the Chl-a concentration decreased in 2015. Although the effort is not high in 2014, the swordfish CPUE increased, since the environmental conditions are within the identified optimum ranges (SST at 28.5 °C, Chl-a at 0.3 mg m⁻³, and SSS at 4.2 kg m⁻³).

4.3. Environmental Variations Affecting the Swordfish Catch

The results showed that the environmental parameters and swordfish catch rates have changed seasonally and inter-annually. According to the BRT model (Table 1) and GAMs (Table 2), the major contributing environmental factors affecting the swordfish habitat were SST and Chl-a (primary production). The SSS mass concentration also affects swordfish distribution.

The BoB, the AS, and the ocean region around Sri Lanka are highly productive regions of the world [43]. The coastal areas are much more productive (Figure 6), due to the nutrient input occurring from rivers and the vertical mixing induced by coastal currents [19]. BRT and model 2 of GAM identified wind speed as an influencing factor for swordfish distribution. Wind and SST affect the fish species distribution indirectly since they regulate the vertical pumping of nutrients [44]. An SST drop coincides with the peak of the vertical pumping velocity [44]. The strong monsoon wind triggers the mechanical mixing in the surface layer and invigoration of the subsurface nutrients, which leads to the increase of the Chl-a concentration. The wind stress curl engenders the vertical pumping velocity and that reduces SST, supplying nutrients to the surface layer [44]. Temperature change affects the alteration of plankton health. The authors in [45] described that the biogeochemical parameter (e.g., temperature, oxygen level, and acidity) changes occurring with climate change have led to changes in primary productivity, plankton community structure, and plankton physiology (e.g., growth, and body size) [45].

The relationship of salinity to fish physiology has been identified in many studies. Some studies have found that saltwater intake through ingestion regulates the growth of fish and the osmosensitivity [46]. The central nervous system triggers the salt water intake after detection of the saline level in the fish body. Several hormones, such as, growth hormone [47] and the renin-angiotensin hormone system [48], influence this phenomenon. Behaviors of fish are also regulated by the central nervous system and several hormones, such as insulin, glucagon, adrenalin, Cholecystokinin, Peptide YY, growth hormone, and thyroid hormones [49]. These hormones are involved in growth control and osmoregulatory processes. The increase of plasma sodium levels with external salinity increments triggers the cellular effects on growth [46]. For many species, their food ingestion rate is also influenced by the external water salinity level [46]. Hence the salinity level is a major parameter that affects the growth rate of marine species.

In addition, SST and SSS indirectly affect fish distribution by regulating stratification and circulation. Previous studies mentioned that the mean zonal flow in the North Indian Ocean is westward and supports the westward advection of salt [50]. In the south equatorial currents, there is also a higher zonal surface salt transport, which flows westward year-round. As there is a salinity difference between the AS and the BoB due to the low net freshwater input to the AS and high evaporation, the salty AS waters are pushed northward by the western portion of the cyclonic features off the Somali coastline and also by the currents within the region associated with the West Indian Coastal Currents. The thermodynamic structure of the northern BoB has a significant influence on the regional air-sea interaction due to the thin mixed layers' sensitivity to the surface fluxes [51]. SST changes by 1–2 °C in response to net cooling and heating associated with cycles of the summer monsoon [52]. During the active post-monsoon cyclone season, SST cooling does not occur along the cyclone tracks in the northside of the BoB [51]. Hence storm-induced vertical mixing does not occur due to the warm barrier layer and the large density gradient across the halocline [53]. This phenomenon limits the SST cooling and favors cyclone intensification [54]. The MLD is also affected by the salinity and the SST. MLD is defined as the depth at which the salinity effect on the density variation is equivalent to the variation

of temperature by $\Delta T = 1\text{ }^{\circ}\text{C}$ from the sea surface [51]. Hence, in addition to their direct effect on fish physiology, salinity and SST also affect fish distribution by regulating the primary productivity through nutrient upwelling [55].

In this study, it was identified that the swordfish is strongly related to SST between 28 and 28.5 °C. Swordfish larvae occur in all the tropical seas, and their distribution is closely related to SST from 24 °C to 29 °C [56]. Moreover, researchers in reference [4] found that the highest gonadal indices are available in the areas with SSTs ranging between 24 °C and 29 °C [57]. They further mention that the reproductive activity of females is restricted to the warmer epipelagic layers with a deeper thermocline. Moreover, the major fish prey items of swordfish are the nomeid (*Cubiceps pauciradiatus*) and the directmid (*Directmoides parini*) [2]. Additionally, *Sthenoteuthis oualaniensis*, onychoteuthid (*Moroteuthis lonnbergii*), ommastrephid (*Ornithoteuthis volatilis*), and the enoploteuthid (*Ancistrocheirus lesueurii*) are the main cephalopod prey [2]. Previous studies have identified that these prey items are also available within similar temperature ranges and plankton abundant places. For example, the population of purple back flying squid (*Sthenoteuthis oualaniensis*) is high in waters with a SST range between 16 °C and 32 °C [58]. The maximum abundance can be observed within 20 °C to 22 °C [58]. Hence, as well as due to physiological needs, swordfish tend to swim in the identified value ranges of the modeled environmental conditions due to the prey availability.

5. Conclusions

In this study, we showed that 0.3–0.4 mg m⁻³ of Chl-a, 28–28.5 °C SST, and (3–5)10⁻⁸ kg m⁻³ of sea salt surface mass concentration are the optimum conditions for swordfish in the Bay of Bengal, the Sri Lankan ocean region, and the Arabian Sea. Swordfish prefer habitats with these environmental conditions as they fulfill their physiological and phenological needs and host an abundance of prey items. The optimum environmental conditions occur in the eastern region of Sri Lanka, in the Bangladesh and Myanmar coastal regions from June to August, and near Pakistan, the west coast of Sri Lanka, the east coast of India, and around Bangladesh and Myanmar from September to November. The maps, prepared according to the identified optimum environmental condition distribution, can be used to demarcate marine protected areas in order to increase fish recruitment and to make swordfish fisheries sustainable in the future.

Author Contributions: Three authors contributed to this study. T.S.M.E., D.T., and L.O., “conceptualization, T.S.M.E.; methodology, T.S.M.E.; software, T.S.M.E. & D.T.; validation, T.S.M.E. and D.T.; formal analysis, T.S.M.E.; investigation, T.S.M.E.; resources, T.S.M.E. and D.T.; data curation, T.S.M.E.; writing—original draft preparation, T.S.M.E.; writing—review and editing, T.S.M.E., D.T. and L.O.; visualization- T.S.M.E.; supervision, D.T.; project administration, D.T.; funding acquisition, T.S.M.E. and D.T.

Funding: This research was funded by National Natural Sciences Foundation of China (41430968, 41876136), Collaborative Innovation Center for 21st-Century Maritime Silk Road Studies, Guangzhou, China (2015HS05), Chinese scholarship council (2015HS05), Prince Albert II foundation in Monaco and Key Special Project of Southern Marine Science and Engineering Guangdong Laboratory (Guangzhou).

Acknowledgments: We thank to MODIS mission scientists and associated NASA personnel, ERDDAP and Indian Ocean Tuna commission for providing the data. We express our sincere thanks to the reviewers and editors.

Conflicts of Interest: The authors declare no conflict of interest.

Appendix A

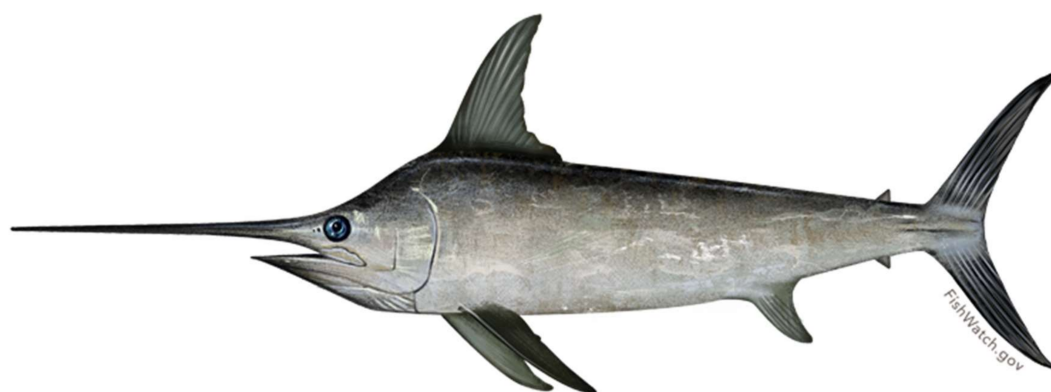


Figure A1. Swordfish [59].

References

1. Food and Agriculture Organization of the United Nations. FAO Fisheries & Aquaculture—Species Fact Sheets—*Xiphias gladius* (Linnaeus, 1758). Fisheries and Aquaculture Department, 2011. Available online: <http://www.fao.org/fishery/species/2503/en> (accessed on 27 May 2019).
2. Potier, M.; Marsac, F.; Cherel, Y.; Lucas, V.; Sabati, R.; Maury, O. Forage fauna in the diet of three large pelagic fishes (lancetfish, swordfish and yellowfin tuna) in the western equatorial Indian Ocean. *Fish. Res.* **2007**, *83*, 60–72. [CrossRef]
3. Poisson, F.; Fauvel, C. Reproductive dynamics of swordfish (*Xiphias gladius*) in the southwestern Indian Ocean (Reunion Island). Part 1: Oocyte development, sexual maturity and spawning. *Aquat. Living Resour.* **2009**, *22*, 45–58. [CrossRef]
4. Mejuto, J.; García-Cortés, B.; Ramos-Cartelle, A. *Iotc 2006-wpb-11 an Overview of Research Activities on Swordfish (Xiphias Gladius) and the by-Catch Species, Caught by the Spanish Longline Fleet in the Indian Ocean*; Report No. 2006; IOTC 2006-WPB-11; IOTC: Victoria, Seychelles; pp. 1–23.
5. *IOTC-WPEB07 2011: Report of the Seventh Session of the IOTC Working Party on Ecosystems and Bycatch*; IOTC: Lankanfinolhu, North Malé Atoll, Republic of Maldives, 2011.
6. Das, P. Indian Deep Sea Fisheries—Its Prospects, Issues and Challenges. *J. Aquacult. Marine Biol.* **2017**, *5*. [CrossRef]
7. Roxy, M.K.; Ritika, K.; Terray, P.; Masson, S. The Curious Case of Indian Ocean Warming. *J. Clim.* **2014**, *27*, 8501–8509. [CrossRef]
8. Anoop, T.R.; Kumar, V.S.; Shanas, P.R.; Johnson, G. Surface Wave Climatology and Its Variability in the North Indian Ocean Based on ERA-Interim Reanalysis. *J. Atmos. Ocean. Technol.* **2015**, *32*, 1372–1385. [CrossRef]
9. Fritz, H.M.; Blount, C.; Albusaidi, F.B.; Al-Harthy, A.H.M. Cyclone Gonu storm surge in the Gulf of Oman. In *Indian Ocean. Tropical Cyclones and Climate Change*; Springer: Dordrecht, The Netherlands, 2010; pp. 255–263.
10. Sumesh, K.G.; Ramesh Kumar, M.R. Tropical cyclones over north Indian Ocean during El-Niño Modoki years. *Nat. Hazards* **2013**, *68*, 1057–1074. [CrossRef]
11. Fogarty, H.E.; Burrows, M.T.; Pecl, G.T.; Robinson, L.M.; Poloczanska, E.S. Are fish outside their usual ranges early indicators of climate-driven range shifts? *Glob. Chang. Biol.* **2017**, *23*, 2047–2057. [CrossRef]
12. Hays, G.; Richardson, A.; Robinson, C. Climate change and marine plankton. *Trends Ecol. Evol.* **2005**, *20*, 337–344. [CrossRef]
13. Lauria, V.; Attrill, M.J.; Pinnegar, J.K.; Brown, A.; Edwards, M.; Votier, S.C. Influence of climate change and trophic coupling across four trophic levels in the Celtic Sea. *PLoS ONE* **2012**, *7*, e47408. [CrossRef]
14. Bornatowski, H.; Angelini, R.; Coll, M.P.; Barreto, R.R.P.; Amorim, A.F. Ecological role and historical trends of large pelagic predators in a subtropical marine ecosystem of the South Atlantic. *Rev. Fish Biol. Fish.* **2017**, *28*, 241–259. [CrossRef]
15. Chang, Y.J.; Sun, C.L.; Chen, Y.; Yeh, S.Z.; DiNardo, G.; Su, N.J. Modelling the impacts of environmental variation on the habitat suitability of swordfish, *Xiphias gladius*, in the equatorial Atlantic Ocean. *ICES J. Mar. Sci.* **2013**, *70*, 1000–1012. [CrossRef]

16. Lan, K.W.; Lee, M.A.; Wang, S.P.; Chen, Z.Y. Environmental variations on swordfish (*Xiphias gladius*) catch rates in the Indian Ocean. *Fish. Res.* **2014**, *166*, 67–79. [[CrossRef](#)]
17. Irby, I.D.; Friedrichs, M.A.M.; Da, F.; Hinson, K.E. The competing impacts of climate change and nutrient reductions on dissolved oxygen in Chesapeake Bay. *Biogeosciences* **2018**, *15*, 2649–2668. [[CrossRef](#)]
18. Jensen, T.G. Arabian Sea and Bay of Bengal exchange of salt and tracers in an ocean model. *Geophys. Res. Lett.* **2001**, *28*, 3967–3970. [[CrossRef](#)]
19. Kay, S.; Caesar, J.; Janes, T. Marine Dynamics and Productivity in the Bay of Bengal. In *Ecosystem Services for Well-Being in Deltas*; Springer International Publishing: Cham, Switzerland, 2018; pp. 263–275.
20. De'ath, G. Boosted trees for ecological modeling and prediction. *Ecology* **2015**, *88*, 243–251. Available online: <http://www.jstor.org/stable/27651085> (accessed on 1 January 2007). [[CrossRef](#)]
21. Elith, J.; Leathwick, J.R.; Hastie, T. A working guide to boosted regression trees. *J. Anim. Ecol.* **2008**, *77*, 802–813. [[CrossRef](#)]
22. Gu, H.; Wang, J.; Ma, L.; Shang, Z.; Zhang, Q. Insights into the BRT (Boosted Regression Trees) Method in the Study of the Climate-Growth Relationship of Masson Pine in Subtropical China. *Forests* **2019**, *10*, 228. [[CrossRef](#)]
23. Lampa, E.; Lind, L.; Lind, P.M.; Bornefalk-Hermansson, A. The identification of complex interactions in epidemiology and toxicology: A simulation study of boosted regression trees. *Environ. Health* **2014**, *13*, 57. [[CrossRef](#)]
24. Wood, S.N. *Generalized Additive Models: An Introduction with R*, 2nd ed.; Chapman and Hall/CRC: London, UK, 2017.
25. Hastie, T.J.; Tibshirani, R.J. *Generalized Additive Models*; Chapman and Hall: London, UK, 1990.
26. Wood, S.N. On confidence intervals for generalized additive models based on penalized regression splines. *Aust. N. Z. J. Stat.* **2006**, *48*, 445–464. [[CrossRef](#)]
27. Su, N.J.; Sun, C.L.; Punt, A.E.; Yeh, S.Z.; DiNardo, G. Modelling the impacts of environmental variation on the distribution of blue marlin, *Makaira nigricans*, in the Pacific Ocean. *ICES J. Mar. Sci.* **2011**, *68*, 1072–1080. [[CrossRef](#)]
28. Friedman, J.H. Greedy function approximation: A gradient boosting machine. *Ann. Stat.* **2001**, *29*, 1189–1232. [[CrossRef](#)]
29. Friedman, J.H.; Meulman, J.J. Multiple additive regression trees with application in epidemiology. *Stat. Med.* **2003**, *22*, 1365–1381. [[CrossRef](#)] [[PubMed](#)]
30. Hamilton, D.F.; Ghert, M.; Simpson, A.H.R.W. Interpreting regression models in clinical outcome studies. *Bone Jt. Res.* **2015**, *4*, 152–153. [[CrossRef](#)] [[PubMed](#)]
31. Golub, G.H.; von Matt, U. Generalized Cross-Validation for Large-Scale Problems. *J. Comput. Graph. Stat.* **1997**, *6*, 1. [[CrossRef](#)]
32. Golub, G.H.; Heath, M.; Wahba, G. Generalized cross-validation as a method for choosing a good ridge parameter. *Technometrics* **1979**, *21*, 215–223. [[CrossRef](#)]
33. Bozdogan, H. Model selection and Akaike's Information Criterion (AIC): The general theory and its analytical extensions. *Psychometrika* **1987**, *52*, 345–370. [[CrossRef](#)]
34. Khoulood, T.; Hedia, B.; Nissaf, B.A.; Marc, S.; Dhafer, M.; Kouni, C.M. Comparative Performance Analysis for Generalized Additive and Generalized Linear Modeling in Epidemiology Methods of Evaluation for Modeling Disease Incidence. *Int. J. Adv. Comput. Sci. Appl.* **2017**, *8*, 418–423.
35. Adeniyi, M.O. Characteristics of total solar radiation in an urban tropical environment. *Int. J. Phys. Sci.* **2012**, *7*, 5154–5161. [[CrossRef](#)]
36. Brown, B.E.; Dunne, R.; Ambasari, I.; Le Tissier, M.D.A.; Satapoomin, U. Seasonal fluctuations in environmental factors and variations in symbiotic algae and chlorophyll pigments in four Indo-Pacific coral species. *Mar. Ecol. Prog. Ser.* **1999**, *191*, 53–69. Available online: <https://www.semanticscholar.org/paper/Seasonal-fluctuations-in-environmental-factors-and-Brown-Dunne/68ef180657a754b4589fc60f3caf420cd1111000> (accessed on 3 May 2019). [[CrossRef](#)]
37. Kumar, G.S.; Prakash, S.; Ravichandran, M.; Narayana, A.C. Trends and relationship between chlorophyll-a and sea surface temperature in the central equatorial Indian Ocean. *Remote. Sens. Lett.* **2016**, *7*, 1093–1101. [[CrossRef](#)]

38. FAO Fisheries & Aquaculture—Fishery Statistical Collections—Global Capture Production. Global Capture Production, 2019. Available online: <http://www.fao.org/fishery/statistics/global-capture-production/en> (accessed on 29 May 2019).
39. IOTC. Data and Statistics[IOTC. Data and Statistics 2019. Available online: <https://www.iotc.org/data-and-statistics> (accessed on 29 May 2019).
40. De Vos, A.; Pattiaratchi, C.B.; Wijeratne, E.M.S. Surface circulation and upwelling patterns around Sri Lanka. *Biogeosciences* **2014**, *11*, 5909–5930. [[CrossRef](#)]
41. Vinayachandran, P.N.; Yamagata, T. Monsoon Response of the Sea around Sri Lanka: Generation of Thermal Domes and Anticyclonic Vortices. *J. Phys. Oceanogr.* **1998**, *28*, 1946–1960. [[CrossRef](#)]
42. Yan, D.; Kai, L.; Wei, Z.; Wei-Dong, Y. The Kelvin Wave Processes in the Equatorial Indian Ocean during the 2006–2008 IOD Events. *Atmos. Ocean. Sci. Lett.* **2015**, *5*, 324–328. [[CrossRef](#)]
43. Dietrich, G.B.Z.Z. *The Biology of the Indian Ocean*, 1st ed.; Gerlach, S.A., Ed.; Springer: Berlin/Heidelberg, Germany, 1973.
44. Tang, D.; Kawamura, H.; Luis, A.J. Short-term variability of phytoplankton blooms associated with a cold eddy in the northwestern Arabian Sea. *Remote Sens. Environ.* **2002**, *81*, 82–89. [[CrossRef](#)]
45. Cheung, W.W.L.; Dunne, J.; Sarmiento, J.L.; Pauly, D. Integrating ecophysiology and plankton dynamics into projected maximum fisheries catch potential under climate change in the Northeast Atlantic. *ICES J. Mar. Sci.* **2011**, *68*, 1008–1018. [[CrossRef](#)]
46. Bœuf, G.; Payan, P. How should salinity influence growth? *Comp. Biochem. Physiol. Part* **2001**, *130*, 411–423.
47. Fuentes, J.; Eddy, F.B. Drinking in Atlantic salmon parrish and smolts in response to growth hormone and salinity. *Comp. Biochem. Physiol. Physiol.* **1997**, *117*, 487–491. [[CrossRef](#)]
48. Perrott, M.N.; Grierson, C.E.; Hazon, N.; Balment, R.J. Drinking behaviour in sea water and fresh water teleosts, the role of the renin-angiotensin system. *Fish Physiol. Biochem.* **1992**, *10*, 161–168. [[CrossRef](#)]
49. Machado, P.B.; Gordo, L.S.; Figueiredo, I. Skate and ray species composition in mainland Portugal from the commercial landings. *Aquat. Living Resour.* **2004**, *234*, 231–234. [[CrossRef](#)]
50. D’Addezio, J.M.; Subrahmanyam, B.; Nyadjro, E.S.; Murty, V.S.N. Seasonal Variability of Salinity and Salt Transport in the Northern Indian Ocean. *J. Phys. Oceanogr.* **2015**, *45*, 1947–1966. [[CrossRef](#)]
51. Seo, H.; Xie, S.P.; Murtugudde, R.; Jochum, M.; Miller, A.J. Seasonal Effects of Indian Ocean Freshwater Forcing in a Regional Coupled Model. *J. Clim.* **2009**, *22*, 6577–6596. [[CrossRef](#)]
52. Mateo, I.; Hanselman, D. *A Comparison of Statistical Methods to Standardize Catch-Per-Unit-Effort of the Alaska Longline Sablefish Fishery*; NOAA Technical Memorandum NMFS-AFSC-269; National Technical Information Service, U.S. Department of Commerce: Springfield, VA, USA, February 2014; pp. 1–71.
53. Sengupta, D.; Ravichandran, M. Oscillations of Bay of Bengal sea surface temperature during the 1998 summer monsoon. *Geophys. Res. Lett.* **2001**, *28*, 2033–2036. [[CrossRef](#)]
54. Yu, L.; McPhaden, M.J. Ocean Preconditioning of Cyclone Nargis in the Bay of Bengal: Interaction between Rossby Waves, Surface Fresh Waters, and Sea Surface Temperatures. *J. Phys. Oceanogr.* **2011**, *41*, 1741–1755. [[CrossRef](#)]
55. Kaimuddin, A.H. Climate Change Impacts on Fish Species Distribution. Approach Using GIS, Models and Climate Evolution Scenario. Ph.D. Thesis, Université de Bretagne Occidentale, Brest, France, June 2016.
56. Taning, X.Y. On the breeding areas of the swordfish (*Xiphias*). *Papers Mar. Biol. Oceanogr.* **1955**, *3*, 438–450.
57. Mejuto, J.; García-Cortés, B. Reproductive activity of swordfish *Xiphias gladius*, in the Atlantic Ocean inferred on the basis of macroscopic indicators. *Rev. Biol. Mar. Oceanogr.* **2014**, *49*, 427–447. [[CrossRef](#)]
58. Jereb, P.; Roper, C.F.E. *Cephalopods of the World: An Annotated and Illustrated Catalogue of Cephalopod Species Known to Date*; Food and Agriculture Organization of the United Nations: Rome, Italy, 2005.
59. Swordfish Retention Limit Adjustment[NOAA Fisheries. NOAA Fisheries is Adjusting the Swordfish General Commercial Permit Retention Limits in the Northwest Atlantic, Gulf of Mexico, and U.S. Caribbean Regions. 2017. Available online: <https://www.fisheries.noaa.gov/bulletin/swordfish-retention-limit-adjustment> (accessed on 14 November 2019).

